The Journal of Immunology

NK Cell Patrolling and Elimination of Donor-Derived Dendritic Cells Favor Indirect Alloreactivity

Kym R. Garrod, Feng-Chun Liu, Luette E. Forrest, Ian Parker, Sang-Mo Kang and Michael D. Cahalan

J. Immunol. 2010;184;2329-2336; originally published online Feb 5, 2010;
doi:10.4049/jimmunol.0902748
http://www.jimmunol.org/cgi/content/full/184/5/2329

The Journal of Immunology is published twice each month by The American Association of Immunologists, Inc., 9650 Rockville Pike, Bethesda, MD 20814-3994.

Print ISSN: 0022-1767 Online ISSN: 1550-6606.

NK Cell Patrolling and Elimination of Donor-Derived Dendritic Cells Favor Indirect Alloreactivity

Kym R. Garrod,* Feng-Chun Liu,† Luette E. Forrest,* Ian Parker,*,‡ Sang-Mo Kang,† and Michael D. Cahalan*,§

Direct presentation of foreign MHC molecules expressed by donor-derived dendritic cells (DCs) has generally been considered the dominant pathway of allorecognition in acute transplant rejection. However, recent studies implicate preferential activation of the indirect pathway by host DCs. The respective importance of each pathway and the mechanisms that determine their relative contributions remain to be clearly established. In this study, using two-photon microscopy, we visualized host NK cell interactions with syngeneic and allogeneic DCs within intact lymph nodes of mice. Upon contact with allogeneic DCs, NK cells formed prolonged interactions that led directly to target cell lysis. This rapid elimination limited the ability of allogeneic DCs to stimulate primary and recall T cell responses. To discriminate whether donor or host DCs are principally involved in presenting Ag derived from allografts, we used CD11c-diphtheria toxoid receptor mice to conditionally ablate CD11c$^+$ DCs and to show that direct presentation by donor DCs is alone insufficient to elicit acute allograft rejection. We thus propose that rapid elimination of allogeneic DCs limits direct Ag presentation and thereby favors the indirect pathway of alloreactivity. ***The Journal of Immunology*****, 2010, 184: 2329–2336.**

Two-photon microscopy permits real-time visualization of living cells within lymphoid organs (1, 2). Two previous studies have imaged the regional distribution and motility of NK cells within the lymph node (LN) (3, 4). Both studies found that NK cells occupy a zone that overlaps the edge of the B cell follicle and extends into the cortical T cell region. However, NK cells were reported by Bajenoff et al. (3) to be immotile, whereas our group showed that untouched NK cells exhibit robust motility with characteristic velocities intermediate between T and B cells (4). Furthermore, we showed that NK cells are capable of recognizing and eliminating foreign B cell targets (4). In this study we sought to further characterize NK cell interaction dynamics using allogeneic dendritic cells (DCs) and to evaluate the role of NK cell patrolling in the context of transplantation.

According to the missing-self hypothesis, NK cells recognize and eliminate cells that fail to express self-MHC molecules (5). In support of this, experimental evidence has demonstrated that NK cells reject allogeneic cells efficiently in vivo (6, 7). NK cells are not able to reject solid organ transplants independent of the adaptive response, but they have been shown to participate in allograft rejection in the context of insufficient costimulation through the CD28-B7 pathway (8, 9).

The cross-talk between innate and adaptive immune pathways is becoming increasingly recognized. In transplantation, much of the focus has been understanding how innate responses can initiate or synergize with adaptive responses in preventing tolerance and effecting allograft rejection. However, little is known about whether innate pathways can downregulate alloimmune responses.

It is generally accepted that T cells can respond to alloantigen via direct or indirect presentation by either donor or host DCs, respectively (10–12). The direct pathway involves T cells directly responding to intact, foreign MHC molecules expressed by donor-derived DCs. In the indirect pathway, in contrast, recipient DCs present donor-derived allopeptides in the context of self-MHC. The precursor frequency of T cells with direct reactivity across a full MHC-mismatch has been estimated to be as high as 5–10%, many orders of magnitude higher than that for conventional Ags (13). This high precursor frequency and the presence of donor DCs within the allograft has led to the assumption that direct presentation is the dominant pathway of allorecognition in acute rejection (14). In contrast, T cells with indirect reactivity have a precursor frequency that is more similar to that of conventional Ags. A prevailing paradigm, therefore, has been that indirect responses are not critical for acute rejection but become more important in chronic alloimmune responses (15–18). Recent studies, however, have shown that T cells with indirect reactivity are disproportionately stimulated after transplantation, allowing a relatively rare population of T cells to become a major component of the acute alloimmune response (19). The exact mechanisms that limit the direct pathway and favor the indirect pathway of alloreactivity are not known.

In this study, we asked whether passenger DCs present within the MHC-disparate organ transplant would be sensitive to NK cell-mediated killing. We hypothesized that NK cell patrolling and elimination of donor DCs would limit direct Ag presentation and thereby contribute to the disproportionate activation of the indirect pathway. To address this hypothesis, we used a combination of functional assays together with two-photon microscopy to

*Department of Physiology and Biophysics, ‡Department of Neurobiology and Behavior, and §Center for Immunology, University of California, Irvine, CA 92697; and †Division of Transplantation, Transplantation Research Laboratory, Department of Surgery, University of California, San Francisco, CA 94143

Received for publication August 19, 2009. Accepted for publication December 29, 2009.

This work was supported by National Institutes of Health Grants T32 AI-060573 (to K.R.G.), GM-48071 (to I.P.), and GM-41514 (to M.D.C.), and University of California San Francisco Liver Center Grant P30 DK026743 (to S.-M.K.).

Address correspondence and reprint requests to Dr. Michael D. Cahalan, 275 Irvine Hall, Box 4561, University of California, Irvine, CA 92697. E-mail address: mcahalan@uci.edu

The online version of this article contains supplemental material.

Abbreviations used in this paper: BM, bone marrow; BMDC, bone marrow-derived dendritic cell; DC, dendritic cell; dLN, draining lymph node; DTH, delayed-type hypersensitivity; DTR, diphtheria toxoid receptor; KLH, keyhole limpet hemocyanin; LN, lymph node; MST, mean survival time; Q-dot, quantum dot.

understand the dynamics and functional consequence of NK–DC interactions in the LN. We show that host NK cells form conjugates and rapidly eliminate allogeneic DCs before they are able to stimulate T cells with direct allospecificity. Moreover, using DC-depleted allografts, we demonstrate that donor DCs are dispensable for acute cardiac allograft rejection in mice. These studies refine our understanding of the interaction between innate and adaptive immunity in alloresponses and begin to define the mechanisms underlying preferential activation of the indirect pathway after transplantation.

Materials and Methods

Mice

C57BL/6 (B6.Ly5.2$^+$), BALB/c, B6.129S7-*Rag1^{tm1Mom}*/J (B6.Rag$^{-/-}$), OT2 (B6, $OVA_{323–339}$ peptide-specific CD4$^+$ TCR transgenic), BALB/c.Thy1.1$^+$, CD11c-diphtheria toxoid receptor (DTR) (B6.FVB-Tg[Itgax-DTR/EGFP]57Lan/J on B6 and C.FVB-Tg[Itgax-DTR/EGFP]57Lan/J on BALB/c background) mice were purchased from the The Jackson Laboratory (Bar Harbor, ME). B6.Ly5.1$^+$ and CB6F1 ($H2^d/H2^b$, [C57BL/6 × BALB/c]F_1) mice were purchased from the National Cancer Institute (Frederick, MD). CD11c-EYFP reporter mice were a gift from M. Nussenzweig (Rockefeller University, New York, NY) (20) and were backcrossed to B6 for 10 generations. 4C mice (B6, CD4$^+$ TCR transgenic with direct alloreactivity toward BALB/c alloantigen) were generated as previously described (21) and maintained on the Rag$^{-/-}$ background. BALB/c.Thy1.1$^+$ × OT2 TCR transgenic mice were bred in our animal facility. Mice were housed in a pathogen-free animal facility, and all procedures were performed in accordance with protocols approved by the animal care and use committee of the University of California (Irvine, CA).

Flow cytometry

Fluorophore-labeled Ab, Fc block (CD16/CD32-purified), NK1.1-depleting Ab (clone PK136, functional grade purified), and isotype controls were purchased from eBioscience (San Diego, CA) and BD Pharmingen (San Diego, CA). Single-cell suspensions were prepared and analyzed by multicolor flow cytometry using BD FACSCalibur (Franklin Lakes, NJ) and CellQuest software (Mountain View, CA).

Bone marrow-derived DC generation and in vivo rejection assay

Bone marrow (BM) was harvested from long bones and plated at 5×10^6/10 ml DC medium (IMDM with 10% FCS (HyClone, Thermo Fischer Scientific), L-glutamine, 50 μM 2-ME, and 30–50 ng/ml GM-CSF) as described previously (22). Bone marrow-derived dendritic cells (BMDCs) were used at 5–8 d following overnight stimulation with 1 μg/ml LPS (*Escherichia coli* 026:B6; Sigma-Aldrich, St. Louis, MO). To quantify allogeneic BMDC rejection, 1–2.5 × 10^6 BMDCs/haplotype were mixed at a 1:1 ratio and stained with 4 μM CFSE (Invitrogen, Carlsbad, CA) at 37°C for 15 min. The reaction was quenched with an equal volume of cold FCS. The 1:1 BMDC mixture was injected into footpads of B6 or Rag$^{-/-}$ recipients. To examine rejection in the absence of continued DC migration, 24 h after the 1:1 BMDC mixture was injected into the pinnae of B6 recipients, the injection site was removed. To examine rejection in the absence of lymphocytes, Rag$^{-/-}$ recipients were treated with 200 μg anti-NK1.1 (PK136) depleting Ab or isotype control. The following day, BMDCs were injected into the footpad of recipient mice, and draining LNs (dLNs) were harvested 36 h later. LNs were finely minced, subjected to collagenase digestion (1 mg/ml collagenase II [Sigma-Aldrich] with 40 μg/ml DNAse I [Worthington, Lakewood, NJ]), stained with Ly5.1 Ab, and analyzed by flow cytometry (FACS). Percent rejection was calculated as follows: 100 (1 − number of allogeneic [Ly5.1$^-$] BMDCs ÷ number of congenic [Ly5.1$^+$] BMDCs).

T cell proliferation assays

CD4$^+$ T cells from (OT2 × BALB/c.Thy1.1$^+$)F_1 mice were purified from LNs and spleen by negative selection using MACS columns (Miltenyi Biotec, Auburn, CA) and stained with 3 μM CFSE at 37°C for 15 min. In vitro proliferation: 1 × 10^6 CD4$^+$ T cells were cocultured in U-bottomed tubes containing 2.5 × 10^5 BMDCs pulsed with 1 μg/ml $OVA_{323–339}$ peptide (AnaSpec, Fremont, CA). After 3 d, cells were stained with Thy1.1 and $V_\beta5$ Ab and analyzed by FACS. In vivo proliferation: 2 × 10^6 CD4$^+$ T cells were adoptively transferred into syngeneic F_1 recipients and rested overnight. The following day, animals were challenged s.c. with 5 × 10^5 BMDCs pulsed with 1 μg/ml $OVA_{323–339}$ peptide. BMDC cultures for in vitro and in vivo experiments were used in parallel. dLNs were harvested at 3 d and FACS analyzed.

Delayed-type hypersensitivity assay

BMDC cultures were pulsed with 10 μg/ml $OVA_{323–339}$ peptide or 100 μg/ml keyhole limpet hemocyanin (KLH) and matured with 1 μg/ml LPS overnight. The following day mice were immunized s.c. with 5 × 10^5 Ag-pulsed BMDCs. After 7 d, mice were challenged with 10 μg $OVA_{323–339}$ peptide or KLH intradermally into the ear pinna. The following day, ear swelling was measured in a blinded manner. The delayed-type hypersensitivity (DTH) reaction was calculated from postchallenge ear width minus baseline ear width prior to Ag injection.

BM reconstitution experiment

B6 mice were exposed to two doses of 500 cGy of total body irradiation at a 3-h interval and immediately following irradiation were injected retro-orbitally with 2 × 10^6 BM cells from CD11c-DTR$^+$ or CD11c-DTR$^-$ donor animals. For 2 d prior and 2 wk following irradiation, animals were maintained on sterile food tablets with trimethoprim sulfa in the formulation as sole diet (Rodent SCIDS MDs; Bio-Serv, Frenchtown, NJ). Four to 6 wk later, animals were anesthetized and exposed to UV light for 30 min to eliminate and reconstitute Langerhans cells (23). Mice were rested for >10 wk following BM reconstitution.

Transplants

BALB/c cardiac allografts were transplanted heterotopically into the abdomen of B6 recipients as described previously (24). Rejection was defined by cessation of cardiac contractions for 2 consecutive days and was confirmed by laparotomy. For NK–DC imaging experiments, donor pinna was painted with FITC (5 mg/ml FITC resuspended in 1:1 acetone-dibutylphthalate) 10 min prior to harvesting skin for transplant. Skin allografts were transplanted onto the dorsal thorax of recipients and secured using sutures placed at the corners (25).

Two-photon imaging

Cell preparations. RBC-lysed (BD Biosciences, San Jose, CA) splenocytes from B6 Rag$^{-/-}$ donors were the source of NK cells for all experiments (4). Some allogeneic BMDC cultures were pulsed overnight with 0.5–1.0 μl quantum dots (Q-dots)/ml; NK cells and Q-dot–labeled, allogeneic BMDCs were stained with 9–10 μM 5-(and 6-((4-chloromethyl)benzyl)amino)tetramethylrhodamine for 30 min; syngeneic BMDC and 4C T cells were stained with 20-40 μM CMAC for 60 min; and some allogeneic BMDCs were stained with 2 μM CFSE for 15 min. All staining procedures were performed at 37°C and quenched with an equal volume of cold FCS. A total of 1–2 × 10^7 NK cells, 2.5–5 × 10^6 BMDCs, and 2–5 × 10^5 4C T cells were adoptively transferred into B6 recipients. To synchronize 4C T cell priming, animals received 200 μg anti-CD62L Ab (Mel-14) just before DC immunization and dLNs were harvested 12 h later.

Imaging. Following adoptive transfer of cells, dLNs (axillary and brachial) were harvested, secured with cyanoacrylate adhesive onto a coverslip (with the cortical region of the LN facing the objective), and placed in an imaging chamber superfused with RPMI 1640 medium bubbled with carbogen (95% O_2/5% CO_2) at 37°C. Two-photon imaging was performed as described previously (1). In brief, multidimensional imaging was performed with femtosecond-pulsed excitation at 780 or 900 nm, or using dual lasers to provide simultaneous excitation at 780 and 900 nm. Dichroic mirrors (510 and 560 nm) were used to split fluorescence emission into three photomultiplier detector channels (blue, green, and red). Successive imaging volumes of 50 μm were acquired at 18- to 21-s intervals. Images were acquired using MetaMorph software, and Imaris Bitplane software was used to process and analyze data. All data are representative of three to six separate experiments.

Statistical analysis

Statistical significance was determined using Student *t* test. Survival data were analyzed by Mann-Whitney test. A value of $p < 0.05$ was considered significant. Data are presented as mean ± SEM.

Results

Allogeneic DCs are killed following prolonged interactions with motile NK cells

We used two-photon microscopy and imaged NK–DC interactions in real-time to compare the behavior of NK cells in the presence of syngeneic or allogeneic BMDCs. Consistent with our previous study

of basal NK cell behavior in LNs (4), NK cells were remarkably motile. They traveled at similar three-dimensional velocities (9.7 ± 0.4 and 10.4 ± 0.3 μm/min, respectively) and exhibited comparable confinement ratios (0.4 ± 0.02; Fig. 1*A*, 1*B*) in the presence of syngeneic and allogeneic BMDCs (Supplemental Videos 1 and 2, respectively). Of note, although motilities were similar, we found NK cells preferentially accumulated in LN draining allogeneic BMDCs 1d following immunization (Supplemental Fig. 1).

Next, we visualized NK cell interaction dynamics with BMDCs and measured the duration of cellular contacts. The vast majority of NK cell associations were transient, regardless of DC haplotype (syn-DCs: 4 min 52 s ± 36 s; allo-DCs: 5 min 54 s ± 42 s; $p = 0.26$; Fig. 1*C*). Occasionally, however, NK cells were seen engaging in productive interactions with allogeneic BMDCs, resulting in cell shrinkage and membrane blebbing of the target DC (Fig. 1*D*; Supplemental Video 3). These lytic interactions (<5% of allogeneic associations) were significantly longer in duration than nonlytic contacts (20 min 20 s ± 4 min 17 s, $p < 0.0001$; Fig. 1*C*). This pattern of stable conjugate formation with MHC-disparate targets is consistent with previous analysis using allogeneic B cell targets (4).

Allogeneic DCs are rejected rapidly from dLNs

Recent evidence demonstrates that NK cells can kill allogeneic DCs within days to weeks after immunization (6, 7). However, their elimination immediately following transfer has not been established. Therefore, the participation of allogeneic DCs in priming early alloimmune responses via direct presentation remains unresolved. To establish the kinetics with which allogeneic DCs are rejected, we adoptively cotransferred CFSE-labeled allogeneic (BALB/c Ly5.2$^+$) and control congenic (C57BL/6 Ly5.1$^+$) BMDCs into the footpad of C57BL/6 (B6 Ly5.2$^+$) recipients. We then quantified the number of transferred DCs in the dLN by FACS (Fig. 2*A*). Within 12 h of transfer, the majority (79 ± 2%; mean ± SEM) of allogeneic BMDCs were eliminated. Interestingly, however, there was no appreciable increase in the percentage of DCs rejected at later times (24 and 48 h) following DC injection (Fig. 2*B*). The

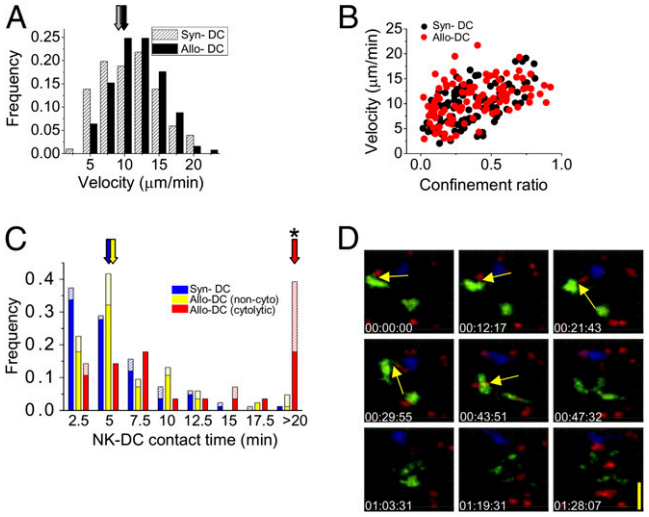

FIGURE 1. Prolonged cognate NK–DC interaction results in cytolysis of allogeneic DCs, visualized in dLNs by two-photon imaging. *A*, Velocities of individual NK cells from LNs under steady-state (syngeneic DCs; hatched bars) and activating (allogeneic DCs; ■) conditions. Arrows indicate mean NK cell velocities (syn-DCs: mean velocity = 9.7 ± 0.4 μm/min, $n = 101$ cells; allo-DCs: mean velocity = 10.4 ± 0.3 μm/min, $n = 125$ cells). *B*, Individual NK cell velocities versus confinement ratios (total length of track divided by the distance between the start and end point) were calculated from DC dLNs (syn-DCs: black dots; allo-DCs: red dots; $n = 101$). *C*, Distribution of NK–DC contact durations. An interaction was defined as a contact lasting >1 min. ■, Exact contact times; hatched bars, cellular interactions that could not be viewed in their entirety (i.e., movie began/ended with cells associated or conjugates moved out of imaging field prior to detachment). Arrows indicate mean NK cell contact time (minutes) with syn-DCs (4 min 52 s ± 36 s; $n = 83$; blue bars) and with allo-DCs when the interaction was noncytolytic (5 min 54 s ± 42 s; $n = 84$; yellow bars) or cytolytic (20 min 20 s ± 4 min 17 s; $n = 28$; red bars). $*p < 0.0001$. *D*, Time-lapse images of a lytic NK–DC interaction (yellow arrows). An individual NK cell (red) is seen engaging an individual allo-DC (green) in the presence of a syn-DC (blue). Original magnification ×20. Scale bar, 10 μm.

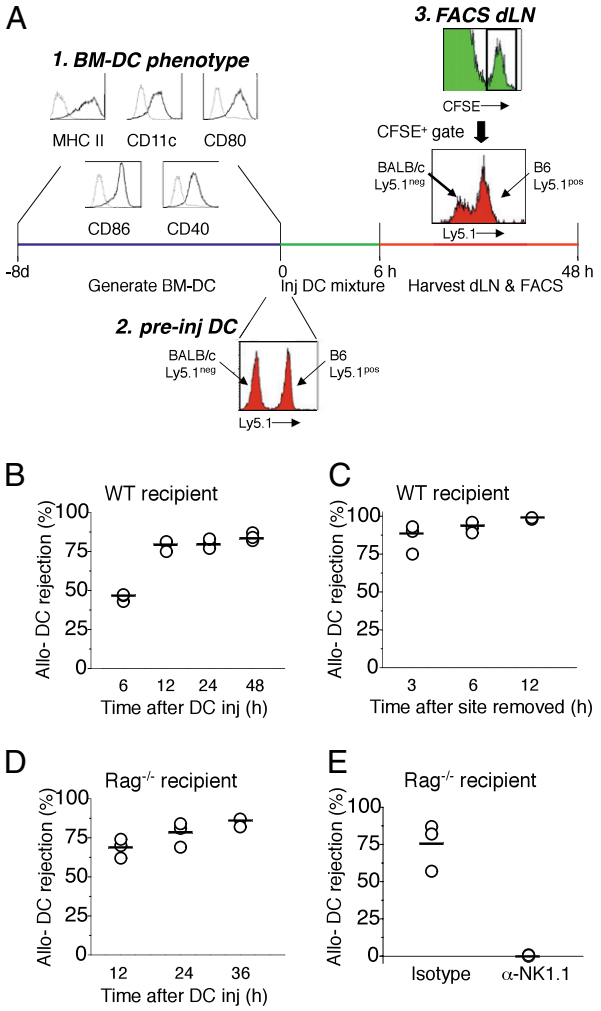

FIGURE 2. NK cells are sufficient to reject allogeneic DCs within dLNs. *A*, Experimental design timeline indicating phenotyping, cell labeling, and recovery of BMDCs from LNs. From left: 1, FACS analysis of BMDCs following LPS-induced maturation showing isotype controls (dashed lines) and DC markers (solid lines) as indicated (*left panel histograms*); 2, CFSE-labeled congenic (B6.Ly5.1$^+$) and allogeneic (BALB/c. Ly5.1$^-$) BMDCs mixed at a 1:1 ratio (*middle panel histogram*); and, 3, following injection into footpads or pinnae, recovery from B6.Ly5.2 WT or Rag$^{-/-}$ LNs. dLNs were harvested and stained with Ly5.1 Ab, and the percentage of allogeneic (Ly5.1$^-$) DCs persisting at the indicated time was determined by FACS analysis using a CFSE$^+$ DC gate (*right panel histograms*). *B* and *D*, Kinetics of allogeneic DC rejection in WT (*B*) and Rag$^{-/-}$ (*D*) recipients. *C*, Rejection of allogeneic DCs in WT recipients following excision of injection site to prevent continued DC migration. *E*, Rejection of DCs in NK cell-replete (isotype) or NK cell-deficient (anti-NK1.1) Rag$^{-/-}$ recipients. Each circle represents an individual mouse ($n = 3$ mice per time point). Data are representative of three (*B*) or two (*C–E*) separate experiments. WT, wild-type.

subset of allogeneic BMDCs that persists over time may represent a population of cells that are inherently resistant to rejection or recent DC immigrants from the periphery that have yet to be rejected. To distinguish between these two possibilities, we first assessed syngeneic BMDC migration. Consistent with previous work (26), individual DCs homed to dLNs gradually and not en masse after transfer (Supplemental Fig. 2). This finding is consistent with the possibility that the subset of allogeneic BMDCs that are not rejected early are recent immigrants. Again consistent with this interpretation, prevention of further DC migration to dLNs by excision of the injection site resulted in almost complete elimination of allogeneic BMDCs within 6 h (Fig. 2*C*).

The rapid kinetics of allogeneic DC rejection suggested an innate response rather than an adaptive primary immune response. Accordingly, the rate of clearance of allogeneic BMDCs was not different in $Rag^{-/-}$ hosts that are NK cell sufficient (Fig. 2*D*) but lack T, B, and NKT cells (4). Furthermore, NK cell depletion with anti-NK1.1 Ab treatment prevented the elimination of allogeneic BMDCs, resulting in comparable survival of congenic and allogeneic BMDCs (Fig. 2*E*). Therefore, NK cells are sufficient for the rapid clearance of allogeneic BMDCs. A less likely explanation of our findings could be an inherent difference in BALB/c compared with B6 BMDCs. To address this possibility, we reevaluated allogeneic BMDC rejection in $Rag^{-/-}$ recipients after anti-NK1.1 Ab treatment. The similar extent of migration for BALB/c and B6 BMDCs in the absence of NK cell-mediated killing (Fig. 2*E*) confirms that the reduced numbers of allogeneic BMDCs in dLNs is due to rejection and cannot be attributed to compromised viability or an inherent defect in BALB/c BMDC migration. Collectively, our data indicate that NK cells are sufficient for the rapid clearance of allogeneic BMDCs.

We next examined the relevance of NK cells in a transplant setting, first assessing DC rejection following skin transplantation. Consistent with our results using adoptively transferred BMDCs, we found the majority of allogeneic $FITC^+$ skin-derived DCs were rejected within 12 h of transplantation (71 ± 6%). Next, we examined the ability of intranodal NK cells to interact with allogeneic $FITC^+$ DCs draining the skin allograft. Again, consistent with our previous data using BMDCs, we found NK cells could directly kill donor-derived DCs within ipsilateral LNs (Supplemental Video 4). Thus, NK cells interact with both BM-derived and donor-derived DCs, preferentially forming stable conjugates with allogeneic targets that result in MHC-mismatched recognition and rejection.

Rejection of allogeneic DCs results in diminished T cell priming and impaired recall responses

Prolonged stimulation is required to induce T cell proliferation and drive differentiation of effector function (27, 28). Thus, we hypothesized that host NK cells may significantly constrain the ability of allogeneic DCs to form stable contacts and to efficiently stimulate T cells. To assess the capacity of allogeneic DCs to prime T cells via the direct pathway, we developed a model system using the (B6 × BALB/c)F_1 hybrid cross. F_1 hybrids are known to reject parental cells through an NK cell-dependent process termed "hybrid resistance" (29). Importantly, hybrid resistance does not depend on CTL or NKT cells (30), thus allowing the functional consequence of NK cell-mediated killing of allogeneic DCs to be assessed. After verifying (B6 × BALB/c)F_1 hybrid resistance to B6 BMDCs (Supplemental Fig. 3), we established a system mimicking direct and indirect presentation using parental B6 BMDCs and syngeneic F_1 BMDCs, respectively (Supplemental Fig. 3). In brief, we adoptively transferred CFSE-labeled (OT2 × BALB/c)F_1 T cells, specific for $OVA_{323–339}$ in the context of $I\text{-}A^b$, into (B6 × BALB/c)F_1 recipients and separately immunized each footpad with either OVA-pulsed F_1 or B6 BMDCs. We harvested dLNs 3 d later and assessed T cell proliferation by CFSE dilution. As expected, immunization with syngeneic F_1 BMDCs elicited robust proliferation (Fig. 3*A*). In stark contrast, direct presentation by parental B6 BMDCs failed to prime cognate T cells (Fig. 3*A*) and resulted in proliferative responses only marginally greater than in control nondraining LNs. Furthermore, although the same number of LN cells was analyzed for each condition; Ag-specific T cells were present in far greater frequency in LN draining syngeneic F_1 BMDCs (Fig. 3*A*). Direct

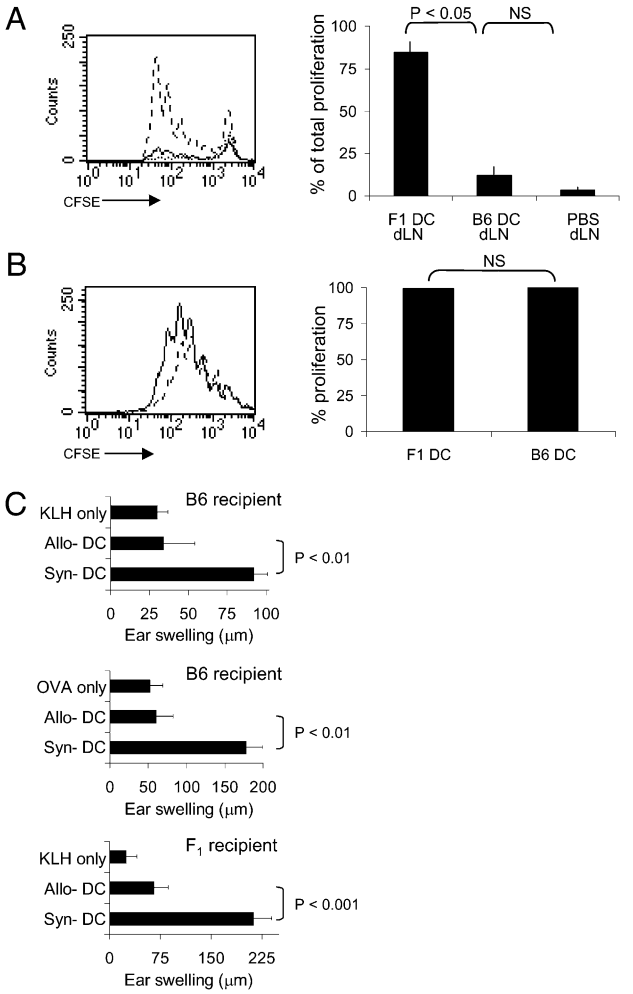

FIGURE 3. Allogeneic DCs fail to prime T cells or establish T cell recall responses through direct presentation in vivo. *A*, In vivo Ag-specific proliferative responses of adoptively transferred CFSE-labeled (OT2 × BALB/c.Thy1.1)F_1 T cells following immunization with syngeneic F1 OVA-pulsed DCs (dashed line), allogeneic B6 OVA-pulsed DCs (solid line), or PBS (dotted line) alone (*left panel histogram*). Percentage of proliferated cells within each dLN was calculated as follows: 100 (number of CFSE-diluted cells within each dLN ÷ total number of CFSE-diluted cells from all dLNs from each individual animal) (*right panel*). Equal numbers of LN cells were collected for each condition (n = 3 mice). *B*, In vitro proliferative responses from CFSE-labeled (OT2 × BALB/c.Thy1.1)F_1 T cells stimulated with syngeneic F1 OVA-pulsed DCs (dashed line) or allogeneic B6 OVA-pulsed DCs (solid line) (*left panel histogram*) and percent proliferation were calculated as follows: 100 (CFSE-diluted cells ÷ the total number of cells) (*right panel*). Experiments performed with parallel DC cultures used in *A*. *C*, DTH responses in B6 (*upper* and *middle panels*) or F_1 (*lower panel*) mice immunized with Ag-pulsed syngeneic or allogeneic DCs. After 7 d, mice were challenged with cognate Ag, and ear swelling was measured the following day (n = 4–5 mice/group). Data are representative of three independent experiments.

presentation by parental B6 BMDCs presumably failed to stimulate activation-induced T cell accumulation and resulted in numbers comparable to control nondraining nodes. These differences noted in vivo do not reflect an inherent defect in B6 Ag-presenting function compared with F_1 BMDCs because in vitro activation using parallel F_1 and B6 BMDC cultures produced similar T cell stimulation profiles (Fig. 3*B*). Moreover, in vivo T cell proliferative responses to parental BMDCs were restored to levels similar as syngeneic BMDCs following NK cell depletion (Supplemental Fig. 3). Therefore, host NK cells are sufficient to limit the ability of allogeneic DCs to efficiently stimulate cognate T cells.

We next investigated T cell recall responses in a system in which both NK cells as well as $CD8^+$ T cells could participate in the recognition and subsequent depletion of allogeneic DCs. We examined the consequence of host-mediated effector cell killing on functional recall responses by assessing DTH following immunization with Ag-pulsed allogeneic compared with syngeneic BMDCs. Consistent with the suggestion that T cell allorecognition occurs through indirect presentation, allogeneic BALB/c BMDCs failed to prime recall responses to a model Ag, KLH, in B6 recipients (Fig. 3*C*, *top panel*). This effect was not KLH specific because a similar absence of ear swelling was observed when mice were immunized with allogeneic, OVA-pulsed BMDCs (Fig. 3*C*, *middle panel*). As expected, parental DCs were equally ineffective at priming functional recall responses in F_1 recipients (Fig. 3*C*, *bottom panel*). These results suggest that, owing to their rapid rate of rejection, allogeneic DCs are unable to sustain a critical threshold of prolonged interaction necessary to directly stimulate either primary or recall T cell responses.

Direct $CD4^+$ alloreactive T cells preferentially form stable conjugates with endogenous DCs

To more directly examine the cellular interactions and processes involved in priming alloreactive T cell responses, we again employed two-photon imaging. First, we developed a system that allowed the simultaneous visualization of allogeneic BMDCs and endogenous DCs by injecting Q-dot–pulsed (31), 5-(and 6-((4-chloromethyl)benzyl)amino)tetramethylrhodamine-colabeled allogeneic BMDCs into CD11c-EYFP reporter mice (20). We included red Q-dot colabeling to provide a method for tracking allogeneic DC alloantigen following host effector cell killing. To assess the ability of allogeneic BMDCs to prime alloreactive T cells via direct presentation we adoptively transferred syngeneic 4C T cells (blue) into B6 CD11c-EYFP (green) recipients and immunized the following day with allogeneic (orange), BALB/c BMDCs (Fig. 4*A*). B6 4C TCR-transgenic T cells were selected for their direct $CD4^+$ alloreactivity against BALB/c ($I\text{-}A^d$) DCs (19). Importantly, it has been previously established that 4C T cells are unresponsive to syngeneic and third-party (C3H) DCs (21). Therefore, 4C T cells can only recognize and respond to allopeptides presented in the context of $I\text{-}A^d$ molecules. As expected under activating conditions, 4C T cells from allogeneic BMDCs immunized dLNs exhibited decreased velocities (4.8 ± 0.3 μm/min) and confinement ratios (0.2 ± 0.02) as compared with unimmunized contralateral control nodes (12.4 ± 0.6 and 0.5 ± 0.03 μm/min, respectively) (Fig. 4*B*). However, when we analyzed individual DC–T cell interactions from immunized LNs, we found that the majority of 4C T cells failed to form stable conjugates with allogeneic BMDCs (9 of 112 conjugates) (Fig. 4*C*). A result that cannot be attributed to an inability to pair with BALB/c cells, as evidenced by the rare allogeneic DC:4C conjugate (Supplemental Video 5). Instead, 4C T cells were largely retained within endogenous CD11c-$EYFP^{dim}$ DC areas. Although the weak fluorescence intensity of CD11c-$EYFP^{dim}$ DCs limited

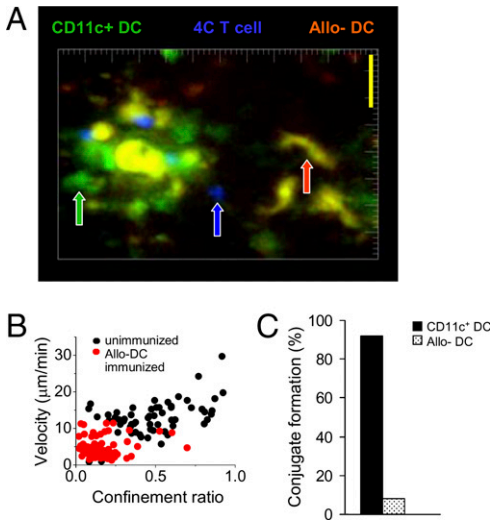

FIGURE 4. In vivo priming of 4C T cells occurs preferentially by indirect presentation. *A*, Snapshot visualization of endogenous CD11c-$EYFP^+$ DCs (green arrow), allogeneic BMDCs (orange arrow) and 4C T cells (blue arrow). Original magnification ×20. Scale bar, 20 μm. *B*, Individual 4C T cell velocities and confinement ratios in LN-draining allogeneic DCs (red dots; $n = 68$) or unimmunized control LNs (black dots; $n = 63$). *C*, 4C T cell interactions with endogenous CD11c-$EYFP^+$ (■; 103 of 112) and allogeneic (dotted bar; 9 of 112) DCs were determined. A 4C:DC conjugate was defined as an individual interaction lasting >10 min.

the ability to distinguish individual interactions, imaging software readily permitted the identification and quantification of endogenous DC:4C conjugates (103 of 112 conjugates) (Fig. 4*C*). Notably, 4C T cells preferentially localized to endogenous DC regions containing allogeneic DC-derived red Q-dots, an indicator for the presence of alloantigen (Supplemental Video 6). Our observation that endogenous DCs can engage T cells with direct alloreactivity is not without precedence and is supported by previous work demonstrating the ability of DCs to acquire and present intact, fully functional, allogeneic MHC molecules (32). These results are consistent with the suggestion that host-mediated immune attack significantly constrains the ability of allogeneic DCs to form stable contacts and to efficiently stimulate cognate T cells. Therefore, even in a system that favors direct presentation, such as the 4C model, the indirect pathway of alloantigen presentation appears to preferentially drive alloreactive T cell activation.

Direct presentation by donor DCs is not sufficient to elicit acute allograft rejection

To further evaluate the relative role of direct and indirect presentation in the setting of transplantation, we assessed rejection of heterotopic heart transplants in the CD11c-DTR transgenic mouse model. The CD11c-DTR model permits the selective and conditional ablation of endogenous $CD11c^+$ DCs (33), allowing us to discern the contribution of direct versus indirect presentation in eliciting allograft rejection. Namely, in the absence of recipient DCs, the role of direct presentation can be assessed. Conversely, in the absence of donor DCs, the role of indirect presentation can be assessed.

Because of lethality associated with the continuous administration of DT to the CD11c-DTR transgenic mice (33, 34), we first generated CD11c-DTR BM chimeras to use as recipients. In our initial experiments, we transplanted BALB/c cardiac allografts into the abdomen of B6 CD11c-DTR^+ BM chimeras and found that grafts were rejected in 6.8 ± 0.5 d (Fig. 5*A*). In contrast, when

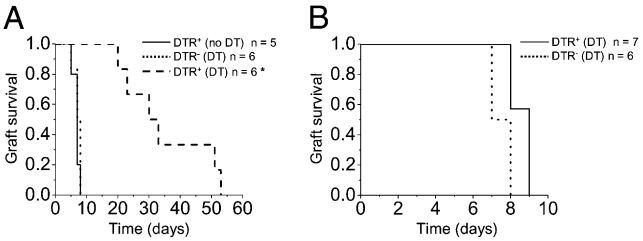

FIGURE 5. Direct presentation by donor DCs is insufficient to trigger acute allograft rejection. *A*, Cardiac survival of WT BALB/c donor allografts placed heterotopically into the abdomen of CD11c-DTR$^+$ (dashed line; mean survival time [MST] = 35 ± 5.7 d; $n = 6$) or CD11c-DTR$^-$ (dotted line; MST = 7.2 ± 0.5 d; $n = 6$) BM chimeras and treated i.p. every other day with 100 ng of DT for the duration of the study. Control CD11c-DTR$^+$ chimeras (solid line; MST = 6.8 ± 0.5 d; $n = 5$) were left untreated (no DT). $*p < 0.0001$. *B*, CD11c-DTR$^+$ (solid line; MST = 8.6 ± 0.2 d; $n = 7$) or CD11c-DTR$^-$ (dotted line; MST = 7.5 ± 0.2 d; $n = 6$) BALB/c donors were treated i.p. with 100 ng of DT. The following day, cardiac allografts were harvested and transplanted heterotopically into the abdomen of DT-treated WT B6 recipients. WT B6 recipients were treated with DT to ensure depletion of any donor-derived passenger DCs that may have remained within the transplanted allograft. MST, mean survival time.

chimeric animals received continuous doses of DT to deplete endogenous DCs, allograft survival was significantly prolonged (35 ± 5.7 d; $p < 0.0001$) (Fig. 5*A*). The slow kinetics with which these grafts were rejected argues against a dominant role for direct presentation in priming allorecognition responses. To rule out any potential involvement for DT in prolonging graft survival, we repeated the experiments using CD11c-DTR$^-$ BM chimeras treated with the same DT regimen as our experimental mice. Similar to the CD11c-DTR$^+$ BM chimeras not receiving DT, these animals rejected their grafts in 7.2 ± 0.5 d (Fig. 5*A*). Additionally, to assess the role of indirect presentation, we transplanted cardiac allografts from DC-depleted BALB/c CD11c-DTR$^+$ donors into wild-type B6 recipients and found that the mice rejected their transplants rapidly (8.6 ± 0.2 d) (Fig. 5*B*). These results suggest that host DCs are more important for acute rejection than donor DCs and are consistent with the concept that donor DCs are not sufficient to provoke an optimal response from allospecific T cells.

Discussion

The relative contribution of direct versus indirect presentation in priming alloreactive T cell responses has yet to be clearly defined. This study reveals cellular dynamics that underlie the indirect pathway of alloantigen presentation by host DCs after transplantation. We used an immunoimaging approach to demonstrate that donor-derived DCs are killed within dLNs as a result of direct NK–DC cytolytic interactions. We found that NK cells actively patrol the LNs with average three-dimensional velocities of 10 μm/min either in the presence or absence of allogeneic DCs and that their motility enables them to rapidly scan the LN microenvironment and eliminate allogeneic DC targets. These three-dimensional NK cell velocities are consistent with our previously reported two-dimensional average velocity of 7 μm/min (4). Furthermore, as in our previous study with foreign B cells (4), NK cells preferentially formed prolonged interactions with allogeneic targets that led to cell lysis. As a result of such interactions with NK cells, allogeneic DCs were eliminated within hours following adoptive transfer or skin transplantation. We examined the functional consequence of this rapid elimination and found that allogeneic DCs were unable to directly stimulate either primary or recall T cell responses. In determining the mechanism by which allorecognition occurs following organ transplantation, we showed that DC-depleted CD11c-DTR$^+$ donor cardiac allografts were rejected with normal kinetics. In contrast, survival of unmanipulated donor hearts into DC-depleted CD11c-DTR$^+$ recipients was prolonged. Taken together, these results validate the patrolling function of rapidly motile NK cells and indicate that direct presentation by donor DCs is dispensable for acute rejection.

Delineation of the mechanisms underlying alloantigen presentation will aid clinical development of tolerogenic interventions to minimize transplant rejection. Traditionally, direct presentation of alloantigens by donor-derived DCs has been a primary focus of transplant immunology and has been regarded as the driving mechanism underlying T cell-mediated allograft rejection. Several lines of evidence have sustained this view. For instance, data from in vitro experiments have demonstrated that the majority of alloreactive T cells respond directly to allogeneic APCs (12, 14). However, the high precursor frequency of T cells with direct alloreactivity does not necessarily indicate that alloreactive T cells are effectively activated through direct presentation in vivo. Further evidence for the primacy of the direct pathway in acute rejection originates from transplant studies demonstrating prolonged survival rates of donor DC-depleted allografts (16, 35, 36). As suggested by Auchincloss et al. (15), however, the defect in allorecognition after donor DC depletion may not just be a consequence of the absence of direct presentation but rather a reflection of the requirement for donor DCs to provide alloantigen to the indirect pathway. That is, donor DCs may act largely as vehicles for transporting sufficient concentrations of allopeptides to endogenous DCs to drive indirect presentation. Therefore, the delay in allograft rejection following donor DC depletion does not necessarily substantiate the premise that direct presentation is required for allograft rejection. Additionally, support for the importance of the direct pathway in allorecognition derives from data indicating normal allograft survival in MHC class II-deficient recipients lacking the indirect pathway of presentation. However, analysis of MHC class II-deficient mice has revealed a profound dysregulation in T cell responsiveness (37–39). Therefore, it has been proposed that MHC class II-deficient mice may use a novel pathway of alloreactivity (39).

Recently, a third pathway of alloantigen presentation termed "semidirect" has been proposed that may account for indirect allorecognition in MHC class II-deficient recipients (32). In the semidirect pathway, recipient DCs acquire and present intact allogeneic MHC:peptide molecules to responding T cells. Thus, MHC class II-deficient cells could acquire Ag-presenting function through the transfer of MHC:peptide complexes from exosomes or directly from short-lived migratory DCs draining the allograft (40, 41). Importantly, the semidirect pathway may also help explain our finding that 4C T cells with direct allospecificity are capable of associating with endogenous DCs, although this issue clearly will require further study.

It is becoming increasingly apparent that prolonged stimulation is essential for T cell activation, acquisition of effector function, and establishment of effective memory (28, 42–47). Celli et al. (28) reported that a contact time of 6 h was required to elicit a single round of T cell division, with maximal proliferation and effector function differentiation achieved only following prolonged DC-T cell interactions persisting >24 h. Therefore, the demonstration of allogeneic DC susceptibility to host-mediated immune attack (6, 7, 40), together with our finding that this occurs within hours of arriving in dLNs, suggests an inability of donor-derived DCs to induce effective T cell stimulation through direct presentation. A straightforward hypothesis, therefore, would be that in the absence of effector cell killing, restoration of direct presentation combined with intact indirect presentation would

result in subsequently enhanced T cell expansion. This is in fact what has been described recently in two studies that used anti–NK1.1-depleting Ab in CD8-deficient mice (7, 48). Interestingly, however, augmented direct alloreactivity did not accelerate allograft rejection. In addition, our suggestion for a predominant role for indirect presentation is further supported by recent evidence using an allospecific TCR transgenic system to examine T cell activation events. Brennan et al. (19) found that following allograft transplantation, T cells were preferentially primed through indirect presentation. Importantly, allospecific T cells with indirect reactivity were enriched in the effector and memory T cell compartments. Therefore, the critical threshold of engagement required to induce robust T cell activation appears to occur preferentially through the indirect pathway of alloantigen presentation.

Our findings provide insight into the role of innate immunity in shaping alloreactivity and emphasize the importance of indirect presentation in generating alloimmune T cell responses. It should be emphasized, however, that although NK cells appear to be important early effectors, this does not exclude overlap with CTL later in the response (49). A suggestion substantiated by our finding that 3 d following DC immunization, NK1.1$^+$ cell depletion in WT animals resulted in comparable levels of allogeneic DC elimination as in isotype-treated controls (unpublished observation). Thus, given sufficient time to develop, CTL may have a complementary role in killing allogeneic DCs. Taken together, our results support the concept that host-mediated immune attack limits direct alloantigen presentation.

In summary, these data refine our understanding of the mechanisms underlying solid organ transplant rejection and may enable more effective tolerance induction protocols to be engineered. In this regard, results from our experiments are in accord with studies indicating that certain tolerizing regimens require indirect presentation (50, 51). Although further investigation is required to assess a potential role for direct presentation in an Ag-experienced recipient containing a complete repertoire of naive as well as memory T cells, our data demonstrate that rapid elimination of donor DCs down-modulates direct Ag presentation, favoring alloreactivity via the indirect pathway. The translation of our findings into a clinically relevant therapeutic intervention emphasizes the adaptation of current immunomodulatory approaches to target the indirect pathway of allopresentation.

Acknowledgments

We thank Tracy Hayden for expert technical assistance. K.R.G. acknowledges generous support from the Arnold and Mabel Beckman Foundation and Achievement Rewards for College Scientists Foundation.

Disclosures

The authors have no conflicts of interest.

References

1. Miller, M. J., S. H. Wei, I. Parker, and M. D. Cahalan. 2002. Two-photon imaging of lymphocyte motility and antigen response in intact lymph node. *Science* 296: 1869–1873.
2. Bousso, P., N. R. Bhakta, R. S. Lewis, and E. Robey. 2002. Dynamics of thymocyte-stromal cell interactions visualized by two-photon microscopy. *Science* 296: 1876–1880.
3. Bajénoff, M., B. Breart, A. Y. Huang, H. Qi, J. Cazareth, V. M. Braud, R. N. Germain, and N. Glaichenhaus. 2006. Natural killer cell behavior in lymph nodes revealed by static and real-time imaging. *J. Exp. Med.* 203: 619–631.
4. Garrod, K. R., S. H. Wei, I. Parker, and M. D. Cahalan. 2007. Natural killer cells actively patrol peripheral lymph nodes forming stable conjugates to eliminate MHC-mismatched targets. *Proc. Natl. Acad. Sci. USA* 104: 12081–12086.
5. Ljunggren, H. G., and K. Kärre. 1990. In search of the "missing self": MHC molecules and NK cell recognition. *Immunol. Today* 11: 237–244.
6. Yu, G., X. Xu, M. D. Vu, E. D. Kilpatrick, and X. C. Li. 2006. NK cells promote transplant tolerance by killing donor antigen-presenting cells. *J. Exp. Med.* 203: 1851–1858.
7. Laffont, S., C. Seillet, J. Ortaldo, J. D. Coudert, and J. C. Guéry. 2008. Natural killer cells recruited into lymph nodes inhibit alloreactive T-cell activation through perforin-mediated killing of donor allogeneic dendritic cells. *Blood* 112: 661–671.
8. Maier, S., C. Tertilt, N. Chambron, K. Gerauer, N. Hüser, C. D. Heidecke, and K. Pfeffer. 2001. Inhibition of natural killer cells results in acceptance of cardiac allografts in CD28$^{-/-}$ mice. *Nat. Med.* 7: 557–562.
9. Kim, J., C. K. Chang, T. Hayden, F. C. Liu, J. Benjamin, J. A. Hamerman, L. L. Lanier, and S. M. Kang. 2007. The activating immunoreceptor NKG2D and its ligands are involved in allograft transplant rejection. *J. Immunol.* 179: 6416–6420.
10. Rogers, N. J., and R. I. Lechler. 2001. Allorecognition. *Am. J. Transplant.* 1: 97–102.
11. Colvin, R. B. 1990. Cellular and molecular mechanisms of allograft rejection. *Annu. Rev. Med.* 41: 361–375.
12. Gould, D. S., and H. Auchincloss, Jr. 1999. Direct and indirect recognition: the role of MHC antigens in graft rejection. *Immunol. Today* 20: 77–82.
13. Suchin, E. J., P. B. Langmuir, E. Palmer, M. H. Sayegh, A. D. Wells, and L. A. Turka. 2001. Quantifying the frequency of alloreactive T cells in vivo: new answers to an old question. *J. Immunol.* 166: 973–981.
14. Liu, Z., Y. K. Sun, Y. P. Xi, A. Maffei, E. Reed, P. Harris, and N. Suciu-Foca. 1993. Contribution of direct and indirect recognition pathways to T cell alloreactivity. *J. Exp. Med.* 177: 1643–1650.
15. Auchincloss, H., Jr., R. Lee, S. Shea, J. S. Markowitz, M. J. Grusby, and L. H. Glimcher. 1993. The role of "indirect" recognition in initiating rejection of skin grafts from major histocompatibility complex class II-deficient mice. *Proc. Natl. Acad. Sci. USA* 90: 3373–3377.
16. Lechler, R. I., and J. R. Batchelor. 1982. Restoration of immunogenicity to passenger cell-depleted kidney allografts by the addition of donor strain dendritic cells. *J. Exp. Med.* 155: 31–41.
17. Benichou, G., P. A. Takizawa, C. A. Olson, M. McMillan, and E. E. Sercarz. 1992. Donor major histocompatibility complex (MHC) peptides are presented by recipient MHC molecules during graft rejection. *J. Exp. Med.* 175: 305–308.
18. Honjo, K., X. Y. Xu, J. A. Kapp, and R. P. Bucy. 2004. Activation and migration of allo-peptide specific TCR transgenic T cells in cardiac allograft rejection. *Cell. Immunol.* 230: 44–55.
19. Brennan, T. V., A. Jaigirdar, V. Hoang, T. Hayden, F. C. Liu, H. Zaid, C. K. Chang, R. P. Bucy, Q. Tang, and S. M. Kang. 2009. Preferential priming of alloreactive T cells with indirect reactivity. *Am. J. Transplant.* 9: 709–718.
20. Lindquist, R. L., G. Shakhar, D. Dudziak, H. Wardemann, T. Eisenreich, M. L. Dustin, and M. C. Nussenzweig. 2004. Visualizing dendritic cell networks in vivo. *Nat. Immunol.* 5: 1243–1250.
21. Brennan, T. V., V. Hoang, K. R. Garrod, F. C. Liu, T. Hayden, J. Kim, and S. M. Kang. 2008. A new T-cell receptor transgenic model of the CD4$^+$ direct pathway: level of priming determines acute versus chronic rejection. *Transplantation* 85: 247–255.
22. Winzler, C., P. Rovere, M. Rescigno, F. Granucci, G. Penna, L. Adorini, V. S. Zimmermann, J. Davoust, and P. Ricciardi-Castagnoli. 1997. Maturation stages of mouse dendritic cells in growth factor-dependent long-term cultures. *J. Exp. Med.* 185: 317–328.
23. Merad, M., M. G. Manz, H. Karsunky, A. Wagers, W. Peters, I. Charo, I. L. Weissman, J. G. Cyster, and E. G. Engleman. 2002. Langerhans cells renew in the skin throughout life under steady-state conditions. *Nat. Immunol.* 3: 1135–1141.
24. Corry, R. J., H. J. Winn, and P. S. Russell. 1973. Heart transplantation in congenic strains of mice. *Transplant. Proc.* 5: 733–735.
25. Billingham, R. E., P. L. Krohn, and P. B. Medawar. 1951. Effect of cortisone on survival of skin homografts in rabbits. *BMJ* 1: 1157–1163.
26. Itano, A. A., S. J. McSorley, R. L. Reinhardt, B. D. Ehst, E. Ingulli, A. Y. Rudensky, and M. K. Jenkins. 2003. Distinct dendritic cell populations sequentially present antigen to CD4 T cells and stimulate different aspects of cell-mediated immunity. *Immunity* 19: 47–57.
27. Mempel, T. R., S. E. Henrickson, and U. H. Von Andrian. 2004. T-cell priming by dendritic cells in lymph nodes occurs in three distinct phases. *Nature* 427: 154–159.
28. Celli, S., F. Lemaître, and P. Bousso. 2007. Real-time manipulation of T cell-dendritic cell interactions in vivo reveals the importance of prolonged contacts for CD4$^+$ T cell activation. *Immunity* 27: 625–634.
29. Snell, G. D., and R. B. Jackson. 1958. Histocompatibility genes of the mouse. II. Production and analysis of isogenic resistant lines. *J. Natl. Cancer Inst.* 21: 843–877.
30. Suzue, K., E. L. Reinherz, and S. Koyasu. 2001. Critical role of NK but not NKT cells in acute rejection of parental bone marrow cells in F_1 hybrid mice. *Eur. J. Immunol.* 31: 3147–3152.
31. Sen, D., T. J. Deerinck, M. H. Ellisman, I. Parker, and M. D. Cahalan. 2008. Quantum dots for tracking dendritic cells and priming an immune response in vitro and in vivo. *PLoS One* 3: e3290.
32. Herrera, O. B., D. Golshayan, R. Tibbott, F. Salcido Ochoa, M. J. James, F. M. Marelli-Berg, and R. I. Lechler. 2004. A novel pathway of alloantigen presentation by dendritic cells. *J. Immunol.* 173: 4828–4837.
33. Jung, S., D. Unutmaz, P. Wong, G. Sano, K. De los Santos, T. Sparwasser, S. Wu, S. Vuthoori, K. Ko, F. Zavala, et al. 2002. In vivo depletion of CD11c$^+$ dendritic cells abrogates priming of CD8$^+$ T cells by exogenous cell-associated antigens. *Immunity* 17: 211–220.

34. Zammit, D. J., L. S. Cauley, Q. M. Pham, and L. Lefrançois. 2005. Dendritic cells maximize the memory CD8 T cell response to infection. *Immunity* 22: 561–570.
35. Lafferty, K. J., A. Bootes, G. Dart, and D. W. Talmage. 1976. Effect of organ culture on the survival of thyroid allografts in mice. *Transplantation* 22: 138–149.
36. Batchelor, J. R., K. I. Welsh, A. Maynard, and H. Burgos. 1979. Failure of long surviving, passively enhanced kidney allografts to provoke T-dependent alloimmunity. I. Retransplantation of (AS X AUG)F_1 kidneys into secondary AS recipients. *J. Exp. Med.* 150: 455–464.
37. Grusby, M. J., and L. H. Glimcher. 1995. Immune responses in MHC class II-deficient mice. *Annu. Rev. Immunol.* 13: 417–435.
38. Fischer, U. B., E. L. Jacovetty, R. B. Medeiros, B. D. Goudy, T. Zell, J. B. Swanson, E. Lorenz, Y. Shimizu, M. J. Miller, A. Khoruts, and E. Ingulli. 2007. MHC class II deprivation impairs CD4 T cell motility and responsiveness to antigen-bearing dendritic cells in vivo. *Proc. Natl. Acad. Sci. USA* 104: 7181–7186.
39. Grusby, M. J., H. Auchincloss, Jr., R. Lee, R. S. Johnson, J. P. Spencer, M. Zijlstra, R. Jaenisch, V. E. Papaioannou, and L. H. Glimcher. 1993. Mice lacking major histocompatibility complex class I and class II molecules. *Proc. Natl. Acad. Sci. USA* 90: 3913–3917.
40. Inaba, K., S. Turley, F. Yamaide, T. Iyoda, K. Mahnke, M. Inaba, M. Pack, M. Subklewe, B. Sauter, D. Sheff, et al. 1998. Efficient presentation of phagocytosed cellular fragments on the major histocompatibility complex class II products of dendritic cells. *J. Exp. Med.* 188: 2163–2173.
41. Montecalvo, A., W. J. Shufesky, D. B. Stolz, M. G. Sullivan, Z. Wang, S. J. Divito, G. D. Papworth, S. C. Watkins, P. D. Robbins, A. T. Larregina, and A. E. Morelli. 2008. Exosomes as a short-range mechanism to spread alloantigen between dendritic cells during T cell allorecognition. *J. Immunol.* 180: 3081–3090.
42. Obst, R., H. M. van Santen, D. Mathis, and C. Benoist. 2005. Antigen persistence is required throughout the expansion phase of a $CD4^+$ T cell response. *J. Exp. Med.* 201: 1555–1565.
43. Scholer, A., S. Hugues, A. Boissonnas, L. Fetler, and S. Amigorena. 2008. Intercellular adhesion molecule-1-dependent stable interactions between T cells and dendritic cells determine $CD8^+$ T cell memory. *Immunity* 28: 258–270.
44. Hugues, S., L. Fetler, L. Bonifaz, J. Helft, F. Amblard, and S. Amigorena. 2004. Distinct T cell dynamics in lymph nodes during the induction of tolerance and immunity. *Nat. Immunol.* 5: 1235–1242.
45. Breart, B., and P. Bousso. 2006. Cellular orchestration of T cell priming in lymph nodes. *Curr. Opin. Immunol.* 18: 483–490.
46. Cahalan, M. D., and I. Parker. 2008. Choreography of cell motility and interaction dynamics imaged by two-photon microscopy in lymphoid organs. *Annu. Rev. Immunol.* 26: 585–626.
47. Miller, M. J., O. Safrina, I. Parker, and M. D. Cahalan. 2004. Imaging the single cell dynamics of $CD4^+$ T cell activation by dendritic cells in lymph nodes. *J. Exp. Med.* 200: 847–856.
48. Coudert, J. D., C. Coureau, and J. C. Guéry. 2002. Preventing NK cell activation by donor dendritic cells enhances allospecific CD4 T cell priming and promotes Th type 2 responses to transplantation antigens. *J. Immunol.* 169: 2979–2987.
49. Laffont, S., J. D. Coudert, L. Garidou, L. Delpy, A. Wiedemann, C. Demur, C. Coureau, and J. C. Guéry. 2006. $CD8^+$ T-cell–mediated killing of donor dendritic cells prevents alloreactive T helper type-2 responses in vivo. *Blood* 108: 2257–2264.
50. Rulifson, I. C., G. L. Szot, E. Palmer, and J. A. Bluestone. 2002. Inability to induce tolerance through direct antigen presentation. *Am. J. Transplant.* 2: 510–519.
51. Yamada, A., A. Chandraker, T. M. Laufer, A. J. Gerth, M. H. Sayegh, and H. Auchincloss, Jr. 2001. Recipient MHC class II expression is required to achieve long-term survival of murine cardiac allografts after costimulatory blockade. *J. Immunol.* 167: 5522–5526.